Engineering Structures 171 (2018) 326–335

Contents lists available at ScienceDirect

Engineering Structures

journal homepage: www.elsevier.com/locate/engstruct

School based optimization algorithm for design of steel frames

Mohammad Farshchin, Mohsen Maniat, Charles V. Camp*, Shahram Pezeshk

Department of Civil Engineering, University of Memphis, Memphis, TN 38152, United States

ARTICLE INFO

Keywords:
Structural design optimization
School-based optimization algorithm
Steel frames
Discrete optimization
Metaheuristic algorithms

ABSTRACT

In this paper, a school-based optimization (SBO) algorithm is applied to the design of steel frames. The objective is to minimize total weight of steel frames subjected to both strength and displacement requirements specified by the American Institute of Steel Construction (AISC) Load Resistance Factor Design (LRFD). SBO is a metaheuristic optimization algorithm inspired by the traditional educational process that operates within a multi-classroom school. SBO is a collaborative optimization strategy, which allows for extensive exploration of the search space and results in high-quality solutions. To investigate the efficiency of SBO algorithm, several popular benchmark frame examples are optimized and the designs are compared to other optimization methods in the literature. Results indicate that SBO can develop superior low-weight frame designs when compared to other optimization methods and improves computational efficiency in solving discrete variable structural optimization problems.

1. Introduction

During the last decades, many optimization techniques have been developed for structural design problems. Among them, metaheuristic algorithms have been proven quite effective. Genetic algorithms (GA) [1–3], ant colony optimization (ACO) [4–8], particle swarm optimization (PSO) [9–12], harmony search (HS) [13,14], charged system search (CSS) [15–17], and colliding bodies optimization (CBO) [18–20] are some of the most popular techniques in structural optimization. Many optimization algorithms have been developed to solve steel frame optimization problems: Camp et al. used ACO [21]; Degertekin employed HS [22]; Kaveh and Talatahari employed imperialist competitive algorithm [23]; Hasancebi and Azad utilized Big Bang–Big Crunch [24]; Kaveh and Talatahari utilized CSS [25]; Togan used teaching-learning-based optimization (TLBO) [26]; Kaveh and Farhoudi proposed dolphin echolocation [27]; Maheri and Narimani used an enhanced HS [28]; Hasançebi and Carbas employed a bat-inspired algorithm [29]; Talatahari et al. utilized an eagle strategy [30]; Carraro et al. employed a search group algorithm [31]; Afzali et al. proposed modified honey bee mating optimization [32]; and Kaveh and Ilchi employed enhanced whale optimization [33].

A common approach in metaheuristic optimization is to randomly generate an initial population of potential solutions and gradually improve the overall fitness of the population in a systematic process. Standard metaheuristic optimization algorithms typically allow only intra-population collaboration; however, a more sophisticated approach is to utilize sets of independent parallel populations that collaborate – extending the explorative capabilities of the algorithm and improving the overall efficiency. An example of this approach is a two-stage optimization algorithm that employs a series of independent metaheuristics to explore different regions of the search space (first stage) and then focus the search on the sub-region with the most promising solutions (second stage) such as eagle strategy [34] and multi-class teaching-learning-based optimization (MC-TLBO) [35]. One of the challenges in the application of two-stage algorithms is the selection and implementation of the first stage termination criterion. The termination criterion introduces parameters that need to be tuned for a specific problem which, in result increases the complexity of the algorithm. To overcome this issue, Farshchin et al. [36] introduced a collaborative multi-population framework that utilized a TLBO algorithm and called it school-based optimization (SBO). SBO extends the simple model of teaching and learning within a classroom modeled by TLBO to a school of numerous collaborative classrooms where teachers can be reassigned to other classrooms and thus share knowledge across the school. Farshchin et al. [36] showed that SBO outperforms basic TLBO in finding low-weight designs of truss structures with frequency constraints in a continuous search space.

In this paper, the effectiveness of SBO in solving discrete optimization problems is investigated. The objective of these optimization problems is to minimize total weight of steel frames subjected to both strength and displacement requirements as specified by the American Institute of Steel Construction (AISC) Load Resistance Factor Design (LRFD) [37]. Three often cited benchmark frame structures are designed to provide a comparison between the performance of SBO and

* Corresponding author.
E-mail address: cvcamp@memphis.edu (C.V. Camp).

https://doi.org/10.1016/j.engstruct.2018.05.085
Received 14 March 2017; Received in revised form 8 May 2018; Accepted 20 May 2018
0141-0296/

other algorithms in the literature. Due to the variety of structural modeling approaches and constraint implementations available in the literature, the analysis and design of these benchmark problems are explained in detail and SBO results are compared to relevant published designs.

2. Optimization algorithm

2.1. Teaching-learning-based optimization

TLBO is a metaheuristic algorithm inspired by the traditional educational process in a class of students [38]. Each student provides a solution for the optimization problem and a student with the best solution will be assigned as the teacher of the classroom. The algorithm considers two main mechanisms for exchanging information in a classroom: between a teacher and a student and inter-student collaboration. These mechanisms are implemented in two different consecutive processes: a Teacher Phase that simulates the influence of a teacher on students; and a Learner Phase that models the cooperative learning among students.

2.1.1. Teacher phase

To simulate this process in an optimization algorithm, the teacher mechanism should be applied across the entire range of the design variables. Each design variable is considered as different subjects in a course. During the Teacher Phase, students try to update their knowledge in each subject based on the information provided by the teacher. In mathematical terms, Teaching Phase is defined by:

$$X_{new}^{k}(j) = X_{old}^{k}(j) \pm \Delta(j) \tag{1}$$

$$\Delta(j) = T_F \times r|M(j) - T(j)| \tag{2}$$

where $X^k(j)$ denotes the jth design variable for the kth design vector, T_F is a teaching factor, r is a uniformly distributed random number within the range of [0,1], $M(j)$ is the mean of the class, and $T(j)$ is state of the teacher. In Eqs. (1) and (2), $\Delta(j)$ indicates the difference between the teacher and the class mean for each design variable (its sign should be selected in such a way that the student always moves toward the teacher). The teaching factor T_F in Eq. (2) is the only adjustable parameter in the TLBO algorithm and is used to specify the size of the local search space around the design. Rao et al. [38] presented data to indicate that a value of $T_F = 2$ is appropriate to balance both the exploration and exploitation aspects of the search in the Teacher Phase; this value is used in this study. At the end of each teaching cycle, the current best student will be used as the teacher of the class for the next iteration. In the original TLBO formulation presented by Rao et al. [38], the mean is given as

$$M(j) = \frac{1}{N}\sum_{k=1}^{N} X^k(j) \tag{3}$$

where N is the size of the population. However, a weighted mean based on the values of student performance provides better results [39]. The fitness-based mean is defined as

$$M(j) = \frac{\sum_{k=1}^{N} \frac{X^k(j)}{F^k}}{\sum_{k=1}^{N} \frac{1}{F^k}} \tag{4}$$

where F^k is the penalized fitness of kth student. The weighted mean puts more emphasis on qualified students and improves the overall performance of the TLBO algorithm.

2.1.2. Learner phase

Interactive learning among students within a classroom can improve individual performance and consequently the overall performance of the class. The procedure for the Learner Phase is given in the following steps:

(a) Randomly select a student, p
(b) Randomly select another student, q such that $p \neq q$
(c) Evaluate the fitness of both students
(d) If $F^p < F^q$ (student p is better than student q), then

$$X_{new}^{p}(j) = X_{old}^{p}(j) + r[X_{old}^{p}(j) - X^q(j)] \tag{5}$$

otherwise

$$X_{new}^{p}(j) = X_{old}^{p}(j) + r[X^q(j) - X_{old}^{p}(j)] \tag{6}$$

In Eqs. (5) and (6), r is a uniformly distributed random number within the range [0,1]. The student p moves towards student q if student q is better than student p ($F^p > F^q$) or away from student q otherwise. The direction and magnitude of the change depends on each student's current position in the search space and the difference in the solution of students' p and q. In either case, student p attempts to improve its state [39].

3. School based optimization (SBO)

SBO is a multi-population metaheuristic algorithm, which extends the single classroom teaching-learning environment with one teacher (TLBO) to a school with multiple classrooms and multiple teachers. In the SBO algorithm, independent classrooms explore the search space simultaneously, each using TLBO; then, at the end of each iteration, a pool of teachers (one teacher from each classroom) is assembled. Before the next iteration, each classroom is assigned a new teacher from the teacher pool allowing the transfer of knowledge between classrooms. Teachers are assigned to classrooms using a roulette wheel selection mechanism based on the teachers' fitness values. In addition, every newly assigned teacher for each classroom should have a better fitness than its current teacher.

Fig. 1 illustrates a flowchart of the SBO algorithm. During each iteration, all students in each classroom c are evaluated (there are a total of N_c classrooms) and the best student (measured by fitness) in each classroom is selected as the classroom's teacher T_c; all teachers are assembled into the teacher pool. Before each subsequent iteration, each classroom selects a new teacher NT_c from the teacher pool using a roulette wheel that is subdivided into segments based on the teachers' fitness values. The teacher assignment mechanism allows the SBO algorithm to use more than one teacher to guide the optimization. In result, this mechanism reduces the likelihood that the algorithm will converge to a local optimum. If for example, a classroom converges to a local optimum, that information will not necessarily be distributed to other classrooms since the performance of that classroom's teacher has a lower probability of being selected as a new teacher. Furthermore, the classroom that developed the local optimum has a chance to be improved from this state with the selection of a better teacher from one of the other classrooms. After each classroom receives a new teacher, TLBO teaching and learning mechanisms are applied to each classroom independently and another round of teacher identification and exchange is initiated. The collaborative interaction between parallel classrooms continues until a termination criterion is met, typically some number of analyses wherein the best solution remains unchanged [21,35,36].

4. Frame optimization

A general objective function for frame optimization problems that only accounts for a structure's weight W is

$$\text{minimize } W = \sum_{i=1}^{N_e} L_i w_n(\eta_i) \tag{7}$$

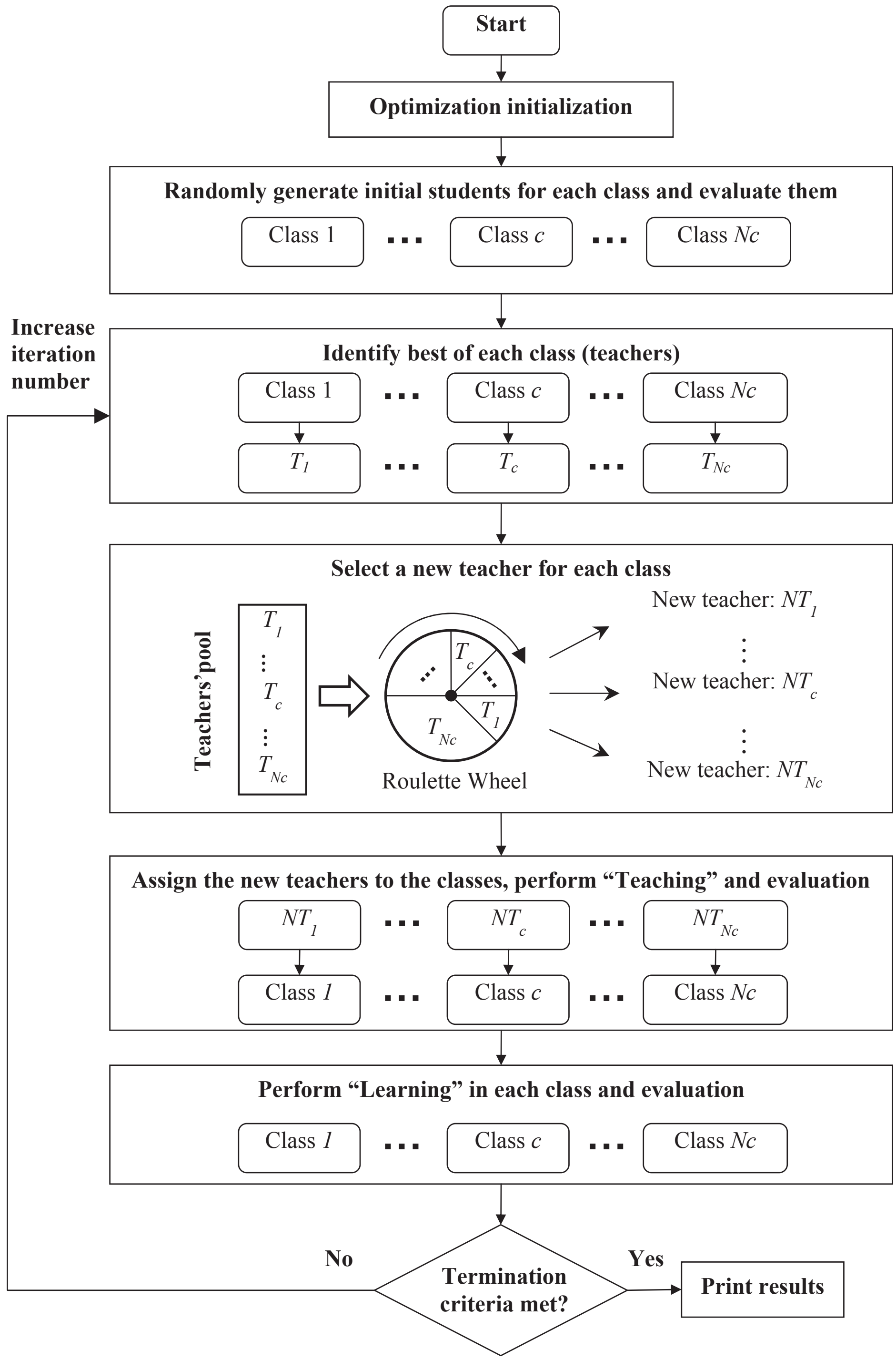

Fig. 1. SBO flowchart.

Table 1
Relationship between index number η and AISC W-shapes [21].

Index number η	Section name	Area (in^2)	Moment of inertia (in^4)
1	W6 × 8.5	2.51	14.8
2	W6 × 9	2.68	16.4
3	W8 × 10	2.96	30.8
.	.	.	.
.	.	.	.
.	.	.	.
266	W36 × 798	235	62,600
267	W14 × 808	237	16,000

where N_e is the number of elements in the frame, L_i is the length of member i, and w_n is the nominal weight of the η_i W-shape for member i chosen from the AISC section database [37]. Table 1 lists the AISC W-shapes sorted by cross-sectional area and referenced by an index η_i [21]. The second value in each W-shape represents the nominal weight of that section. For example, a W24 × 55 is a W-shape nominally weights 55 (lb/ft).

The AISC-LRFD [37] specifications include strength and stability requirements combined with displacement limits (allowable interstory drift). These constraints are enforced on an unconstrained optimization problem by penalizing the objective function. The penalized structural weight F is

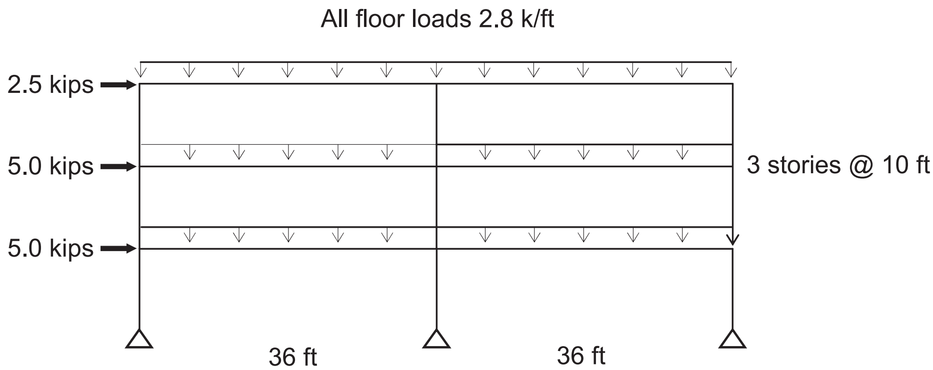

Fig. 2. Geometry and applied loading for two-bay, three-story frame.

Table 2
Designs for two-bay, three-story frame.

Element group	Optimum [21]	GA [45]	ACO [21]	Present work
Beam	W24 × 62	W24 × 62	W24 × 62	W24 × 62
Column	W10 × 60	W10 × 60	W10 × 60	W10 × 60
Weight (lb)	18,792	18,792	18,792	18,792
Mean (lb)	–	22,080	19,163	18,792
Standard deviation (lb)	–	5818	1693	0
Number of analyses	–	900	880	502
Number of runs	–	30	100	100
% optimal found	–	20%	84%	100%

$$F = W(1 + C)^{\varepsilon} \tag{8}$$

where ε is the penalty function exponent which is a positive value usually greater than 1, and C is a constraint violation function defined by Pezeshk et al. [45] as

$$C = \sum_{i=1}^{N_e} C_i^{\sigma} + \sum_{i=1}^{N_s} C_i^{d} + \sum_{i=1}^{N_c} C_i^{\mathrm{I}} \tag{9}$$

where C_i^{σ}, C_i^{d}, and C_i^{I} are the constraint violations for stress, displacement, and the LRFD interaction formulas, N_s is the number of stories, and N_c is the number of beam columns.

In general, the penalty function C may be expressed as

$$C_i = \begin{cases} 0 & \text{if } \alpha_i \leqslant 0 \\ \alpha_i & \text{if } \alpha_i > 0 \end{cases} \tag{10}$$

where α_i is a measure of the degree of constraint violation.

For stress constraints, α_i^{σ} is defined as

$$\alpha_i^{\sigma} = \frac{|\sigma_i|}{|\sigma_i^{a}|} - 1 \tag{11}$$

where σ_i is the stress in element i and σ_I^{a} is the allowable stress in element i.

For interstory drift constraints, α_i^{d} is defined as

$$\alpha_i^{d} = \frac{|d_i|}{|d_i^{a}|} - 1 \tag{12}$$

where d_i is the interstory displacement in story i and d_i^{a} is the allowable interstory displacement (story height)/300 [37]. It should be noted that this constraint is changed to accommodate different displacement constraints as discussed in one of the example problems.

For the LRFD interaction formula constraints (Equation H1-1a, b [37]), α_i^{I} is defined as

$$\alpha_i^{\mathrm{I}} = \frac{P_u}{2\phi_c P_n} + \left(\frac{M_{ux}}{\phi_b M_{nx}} + \frac{M_{uy}}{\phi_b M_{ny}}\right) - 1 \qquad \text{for} \quad \frac{P_u}{\phi_c P_n} < 0.2 \tag{13}$$

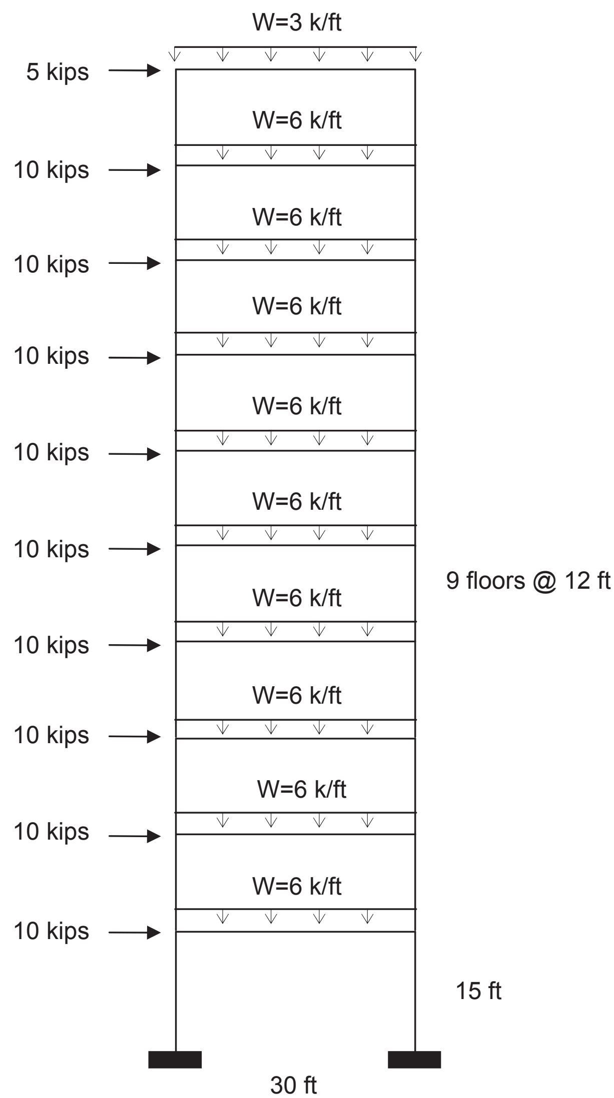

Fig. 3. Geometry and applied loading for one-bay, ten-story frame.

$$\alpha_i^{\mathrm{I}} = \frac{P_u}{\phi_c P_n} + \frac{8}{9}\left(\frac{M_{ux}}{\phi_b M_{nx}} + \frac{M_{uy}}{\phi_b M_{ny}}\right) - 1 \qquad \text{for} \quad \frac{P_u}{\phi_c P_n} \geqslant 0.2 \tag{14}$$

where P_u is the required axial strength (tension or compression); P_n is the nominal axial strength (tension or compression); ϕ_c is the resistance factor ($\phi_c = 0.90$ for tension, $\phi_c = 0.85$ for compression); M_{ux} and M_{uy} are the required flexural strengths in the x and y directions, respectively; M_{nx} and M_{ny} are the nominal flexural strengths in the x and y

Table 3
Designs for one-bay, ten-story frame.

Element group	Case 1		Case 2			
	GA [45]	Present work	ACO [21]	TLBO [26]	SGA [31]	Present work
Column 1-2S	W14 × 233	W14 × 233	W14 × 233	W14 × 233	W14 × 233	W14 × 233
Column 3-4S	W14 × 176	W14 × 176	W14 × 176	W14 × 176	W14 × 176	W14 × 176
Column 5-6S	W14 × 159	W14 × 159	W14 × 145	W14 × 145	W14 × 132	W14 × 145
Column 7-8S	W14 × 99	W14 × 99	W14 × 99	W14 × 99	W14 × 99	W14 × 99
Column 9-10S	W12 × 79	W14 × 61	W12 × 65	W12 × 65	W14 × 68	W14 × 61
Beam 1-3S	W33 × 118	W33 × 118	W30 × 108	W30 × 108	W30 × 108	W30 × 108
Beam 4-6S	W30 × 90	W30 × 90	W30 × 90	W30 × 90	W30 × 90	W30 × 90
Beam 7-9S	W27 × 84	W27 × 84	W27 × 84	W27 × 84	W27 × 84	W27 × 84
Beam 10S	W24 × 55	W18 × 46	W21 × 44	W21 × 44	W21 × 50	W18 × 46
Weight (lb)	65,136	64,002	62,562	62,562	62,262	62,430
Mean (lb)	–	65,880	63,308	–	65,257	63,244
Standard eviation (lb)	–	832.95	684	–	1,328.8	706.84
Number of analyses	3000*	12,691	8300	4000	7980	11,677
Number of runs	–	100	100	–	100	100

* Estimated value.

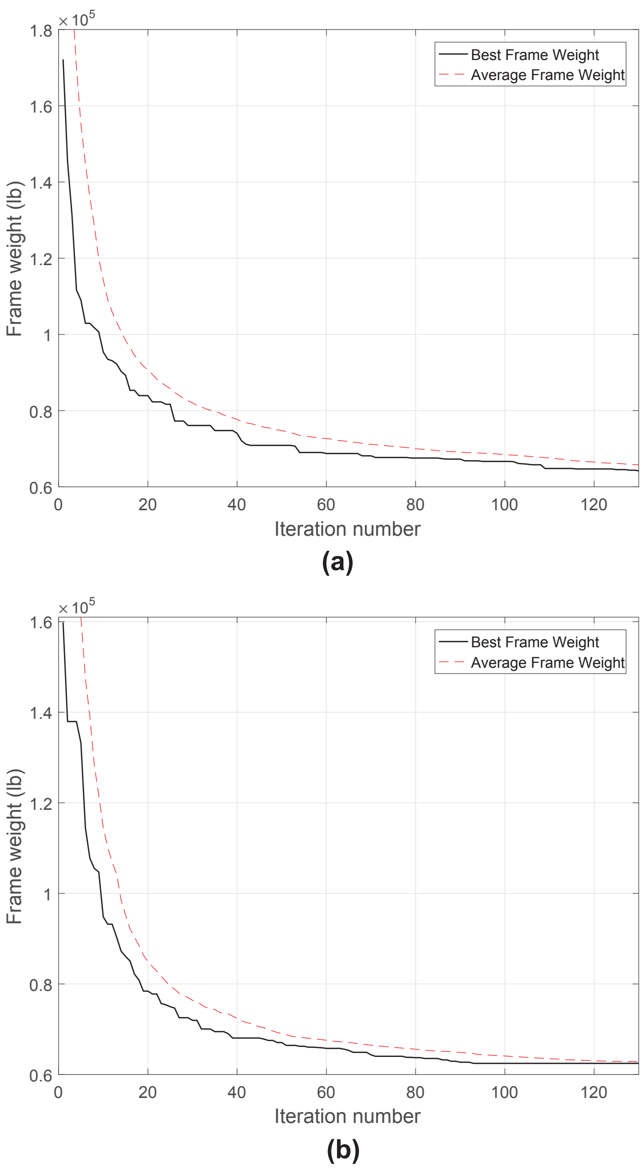

Fig. 4. Typical convergence history of one-bay, ten-story frame for (a) case 1 and (b) case 2.

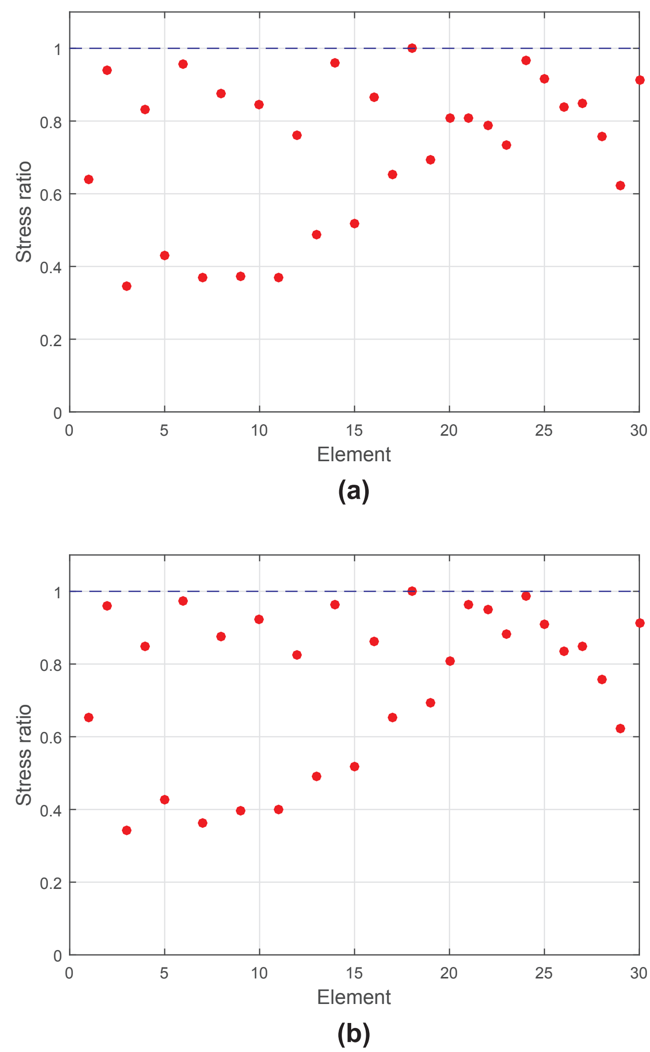

Fig. 5. Stress ratio for members of one-bay, ten-story frame for (a) case 1 and (b) case 2.

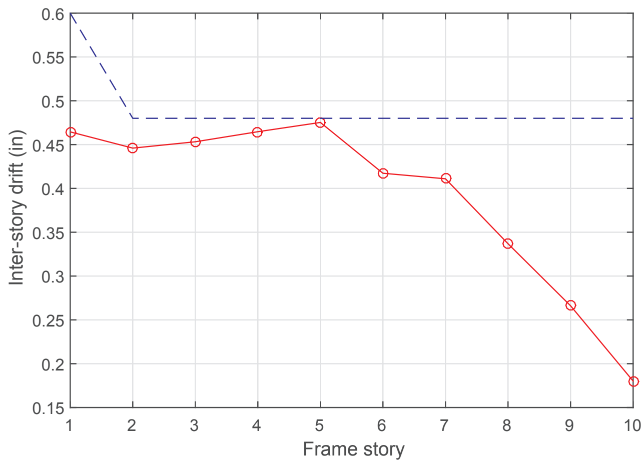

Fig. 6. Interstory drift for one-bay, ten-story frame.

directions (for two-dimensional structures, $M_{ny} = 0$); and ϕ_b is the flexural resistance reduction factor ($\phi_b = 0.90$). The nominal tensile and compressive strengths P_n are

$$P_n = A_g F_y \tag{15}$$

$$P_n = A_g F_{cr} \tag{16}$$

where A_g is the cross-sectional area of the member, F_y is the yield stress of steel, and F_{cr} is given as

$$F_{cr} = \begin{cases} (F_y)0.658^{\frac{F_y}{F_e}} & \text{if } \frac{KL}{r} \leqslant 4.71\sqrt{\frac{E}{F_y}} \\ 0.877F_e & \text{otherwise} \end{cases} \tag{17}$$

where E is the modulus of elasticity, K is the effective length factor, L is the member length, r is the radius of gyration, and F_e is the Euler buckling load given as:

$$F_e = \frac{\pi^2 E}{(\frac{KL}{r})^2} \tag{18}$$

Nominal flexural strength for doubly symmetric compact I-shaped members is calculated based on Section F2 in the AISC manual [37]. The effective length factor K, for unbraced frames is approximated from the following [42]

$$K = \sqrt{\frac{1.6G_A G_B + 4.0(G_A + G_B) + 7.5}{G_A + G_B + 7.5}} \tag{19}$$

where G_A and G_B are relative stiffness ratios of a member with end nodes A and B. The value of G at each node is calculated as

$$G = \frac{\sum (I_{column}/L_{column})}{\sum (I_{beam}/L_{beam})} \tag{20}$$

where I and L are the moment of inertia and length of the members, respectively.

According to AISC-LRFD specifications [37], the required first order flexural and axial strengths should be amplified to account for the second order effects in structures as follows

$$M_r = B_1 M_{nt} + B_2 M_{lt} \tag{21}$$

$$P_r = P_{nt} + B_2 P_{lt} \tag{22}$$

where M_r and P_r are the required second order flexural and axial strengths of all members, respectively; B_1 and B_2 are the multipliers to account for $P-\delta$ and $P-\Delta$ effects, respectively; M_{nt} and P_{nt} are the first order moments and axial forces due to lateral translation of the structure, respectively; M_{lt} and P_{lt} are the first order moments and axial forces with the structure restrained against lateral translation, respectively. To be consistent with other frame designs in the literature, only $P-\delta$ effects are considered in this study. The values of B_1 and B_2 are calculated as [37]:

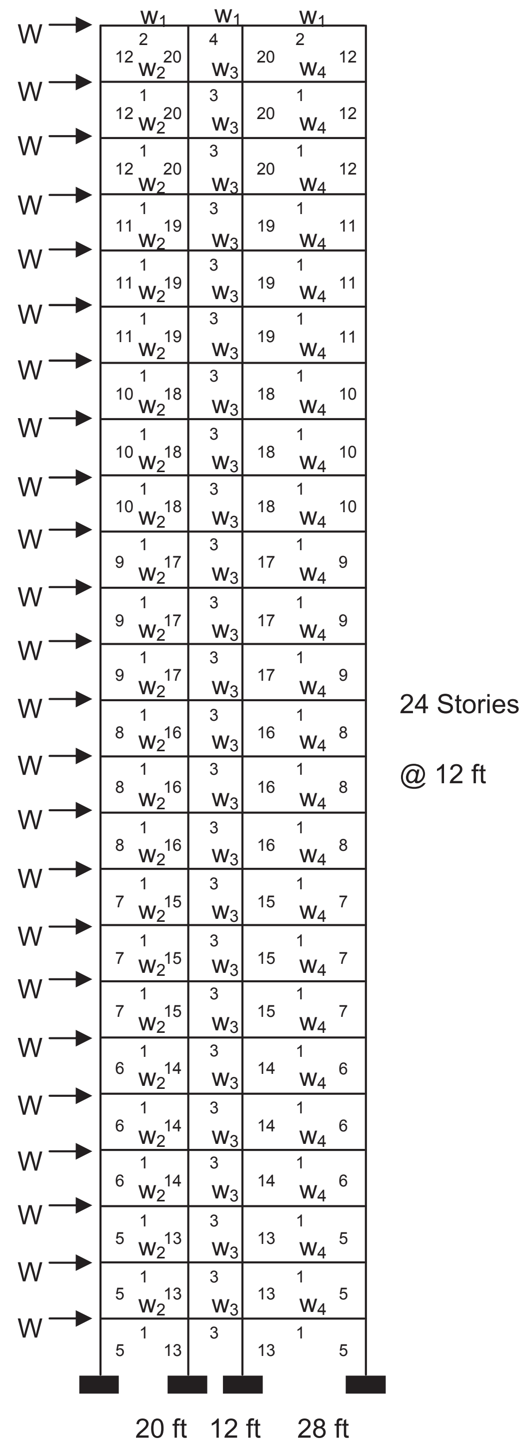

Fig. 7. Geometry and applied loading for three-bay, twenty-four-story frame.

$$M_r = B_1 M_{nt} + B_2 M_{lt} \tag{23}$$

with

$$B_1 = C_m \frac{1}{1 - P_u/P_{e1}} \tag{24}$$

where P_{e1} is the Euler buckling load with $K = 1$ and C_m is

Table 4
Designs for three-bay, twenty-four-story frame.

Element group	Case 1		Case 2				
	ACO [21]	Present work	HS [22]	TLBO [26]	ESDE [30]	EWOA [33]	Present work
1	W30 × 90	W30 × 90	W30 × 90	W30 × 90	W30 × 90	W30 × 90	W30 × 90
2	W8 × 18	W8 × 18	W10 × 22	W8 × 18	W21 × 55	W10 × 30	W8 × 18
3	W24 × 55	W24 × 55	W18 × 40	W24 × 62	W21 × 48	W24 × 55	W21 × 48
4	W8 × 21	W6 × 8.5	W12 × 16	W6 × 9	W10 × 45	W6 × 8.5	W6 × 8.5
5	W14 × 145	W14 × 193	W14 × 176	W14 × 132	W14 × 145	W14 × 159	W14 × 152
6	W14 × 132	W14 × 145	W14 × 176	W14 × 120	W14 × 109	W14 × 99	W14 × 120
7	W14 × 132	W14 × 120	W14 × 132	W14 × 99	W14 × 99	W14 × 120	W14 × 109
8	W14 × 132	W14 × 82	W14 × 109	W14 × 82	W14 × 145	W14 × 74	W14 × 74
9	W14 × 68	W14 × 53	W14 × 82	W14 × 74	W14 × 109	W14 × 74	W14 × 82
10	W14 × 53	W14 × 53	W14 × 74	W14 × 53	W14 × 48	W14 × 43	W14 × 43
11	W14 × 43	W14 × 38	W14 × 34	W14 × 34	W14 × 38	W14 × 30	W14 × 34
12	W14 × 43	W14 × 22	W14 × 22	W14 × 22	W14 × 30	W14 × 22	W12 × 19
13	W14 × 145	W14 × 120	W14 × 145	W14 × 109	W14 × 99	W14 × 90	W14 × 109
14	W14 × 145	W14 × 132	W14 × 132	W14 × 99	W14 × 132	W14 × 120	W14 × 109
15	W14 × 120	W14 × 120	W14 × 109	W14 × 99	W14 × 109	W14 × 90	W14 × 99
16	W14 × 90	W14 × 109	W14 × 82	W14 × 90	W14 × 68	W14 × 99	W14 × 99
17	W14 × 90	W14 × 99	W14 × 61	W14 × 68	W14 × 68	W14 × 68	W14 × 68
18	W14 × 61	W14 × 61	W14 × 48	W14 × 53	W14 × 68	W14 × 61	W14 × 61
19	W14 × 30	W14 × 34	W14 × 30	W14 × 34	W14 × 61	W14 × 43	W14 × 34
20	W14 × 26	W12 × 19	W14 × 22	W14 × 22	W14 × 22	W14 × 22	W14 × 22
Weight (lb)	220,416	216,306	214,896	203,124	212,988	203,490	202,422
Mean (lb)	229,555	224,310	222,620	–	–	208,648	209,560
Standard deviation (lb)	4561	6855	–	–	–	–	7052
Number of analyses	15,500	14,817	14,651	12,000	12,500	18,820	14,572
Number of runs	100	100	100	–	20	20	100

$$C_m = 0.6 - 0.4\frac{M_1}{M_2} \tag{25}$$

where M_1 and M_2, calculated from a first-order analysis, are the smaller and larger moments, respectively. The term B_2 accounts for the $P-\delta$ effect and is calculated for each floor as

$$B_2 = \frac{1}{1-\frac{1}{0.85}\frac{\Delta_h}{h}\frac{P_{story}}{H}} \tag{26}$$

where Δ_h is the first order drift due to lateral forces, h is the height of story, P_{story} is the total vertical load, and H is the shear force due to the lateral loads.

5. Design examples

In this section, SBO is applied to a series of benchmark steel frame design problems. Since different approaches are presented for modeling, analysis, and design of these benchmark problems in the literature, the variations are categorized into different cases and relevant solutions are compared. Different researchers have identified infeasibility of some of the designs provided in the literature [31,40]. In this study, only feasible designs, ones with no constraint violation, are considered.

Since there are no adjustable parameters associated with SBO, the only algorithmic parameter is the size of the population. As suggested by Farshchin et al. [36], a population of five classes, each with ten students, resulting in a total population of 50 is appropriate for these size of structural design optimization problems. In addition, the penalty function exponent ε, defined at Eq. (8), is set equal to 2 for all examples. For the purpose of comparing the number of analyses required to generate designs with other optimization methods, SBO uses the convergence criterion proposed by Camp et al. [21]; wherein, the algorithm is terminated when best solution remains unchanged for 2000 analyses.

5.1. Two-bay three-story frame design

Fig. 2 shows the topology and loading conditions of a two-bay, three-story frame consisting of 15 members originally presented by Wood et al. [41]. Numerous researchers have developed design procedures for this frame that satisfy AISC-LRFD specifications while minimizing the structural weight [22,26,28,42,43]. Displacement constraints are not considered in this example. The material has a modulus of elasticity $E = 29{,}000$ ksi and a yield stress of $F_y = 36$ ksi. Imposed fabrication conditions require that all six beams be the same W-shape chosen from the 267 available W-shapes, listed in Table 1, and all nine columns are identical and restricted to W10 sections (18 W-shapes). For each column, the effective length factor K_x is calculated as for a sway-permitted frame using a simplified form of the transcendental equations [44] and the out-of-plane effective length factor is $K_y = 1.0$. Each column is considered unbraced along its length and the unbraced length for each beam member is specified as 1/6 of the span length. The size of the resulting search space is approximately 4806 designs.

An exhaustive search found the optimal weight of the two-bay, three-story frame to be 18,792 lb. [21]. SBO required only 502 (but as few as 200) frame analyses to converge to the optimum solution. In 100 independent runs, SBO always obtains the optimum solution; therefore, the mean value is equal to the optimum solution and the standard deviation is zero. For comparison, a GA [45], over 30 runs, found the optimal design in 20% of the time with an average weight of 22,080 lb. and a standard deviation of 5818 lb. and an ACO algorithm [21], over 100 runs, developed the optimal design 84% of the time with an average weight of 19,163 lb. and a standard deviation of 1693 lb. Table 2 summarizes designs developed using SBO, a GA [45], and ACO [21]. While this is a simple frame design, the results indicate that SBO is both computationally efficient and less likely to be influenced by a local optimum or the initial distribution of the search population.

5.2. One-bay, ten-story frame

Fig. 3 shows the topology and loading conditions for a one-bay, ten-story frame consisting of 30 members. This frame is designed following

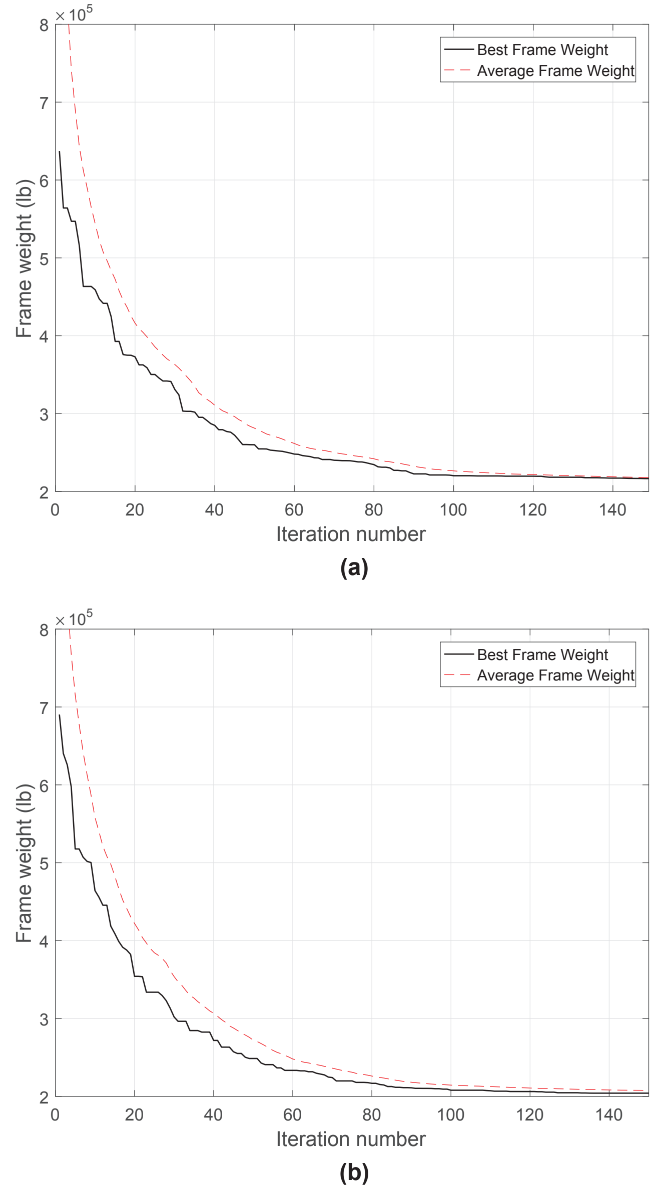

Fig. 8. Typical convergence history of three-bay, twenty-four-story frame for (a) case 1 and (b) case 2.

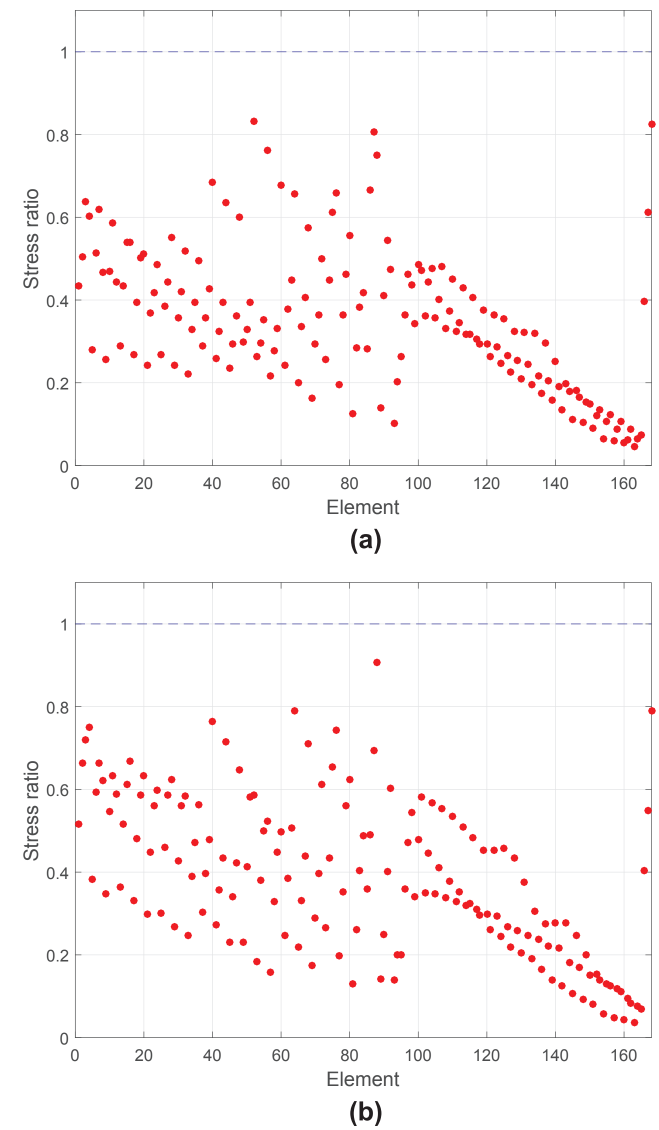

Fig. 9. Stress ratio for members of three-bay, twenty-four-story frame for (a) case 1 and (b) case 2.

the AISC-LRFD specification [37]. The material has a modulus of elasticity $E = 29{,}000$ ksi and a yield stress of $F_y = 36$ ksi. The effective length factors of the members are calculated as $K_x \geq 1.0$ for a sway-permitted frame using a simplified form of the transcendental equations [44] and the out-of-plane effective length factor is specified as $K_y = 1.0$. Each column is considered unbraced along its length and the unbraced length for each beam member is specified as 1/5 of the span length. The element grouping results in 4 beam sections and 5 column sections. Each of the four beam element groups is selected from all 267 W-shapes, listed in Table 1, and the five column element groups are limited to W14 and W12 sections (66 W-shapes). The size of the resulting search space is approximately 6.36 (10^{18}) designs.

There are two approaches to enforcing the displacement constraints in the literature: Case 1, limits the interstory drift for all stories to (story height)/300; while Case 2, only limits the displacement of the roof to (frame height)/300. In this study, both cases are considered and the generated designs are compared to other relevant optimization results reported in the literature.

For statistical purposes, both cases are optimized 100 times. For Case 1, SBO found a lighter design than the GA [45]; however, more analyses are performed. In Case 2, SBO found a lighter design than both ACO [21] and TLBO [26]. The SBO frame was slightly heavier than the design using SGA [31]; however, element number 10 of the SGA design slightly violates stress ratio ($\alpha_i^{\sigma} = 1.014$). In addition, statistical results show that over 100 runs, SBO has an average weight that is 3.1% lighter with a standard deviation that is 47% lower than designs developed with a SGA [31]. Table 3 summarizes the design optimization performance for SBO, GA [47], ACO [21], TLBO [26], and SGA [31]. Fig. 4 shows the convergence history plots for the SBO algorithm for both cases. Fig. 5 shows stress ratio values for each member in the frame for both displacement cases. The maximum stress ratio for Case 1 is $\alpha_i^{\sigma} = 0.9998$ and for Case 2 is $\alpha_i^{\sigma} = 0.9999$; both cases are controlled by element 26 (the beam on the 6th story). Fig. 6 shows the interstory drift for Case 2; the maximum drift of 0.495 in. is associated with the 5th story.

5.3. Three-bay, twenty four-story frame

Fig. 7 shows the topology and the service loading conditions for a three-bay, twenty-four-story frame consisting of 168 members originally designed by Davison and Adams [46]. The loads are

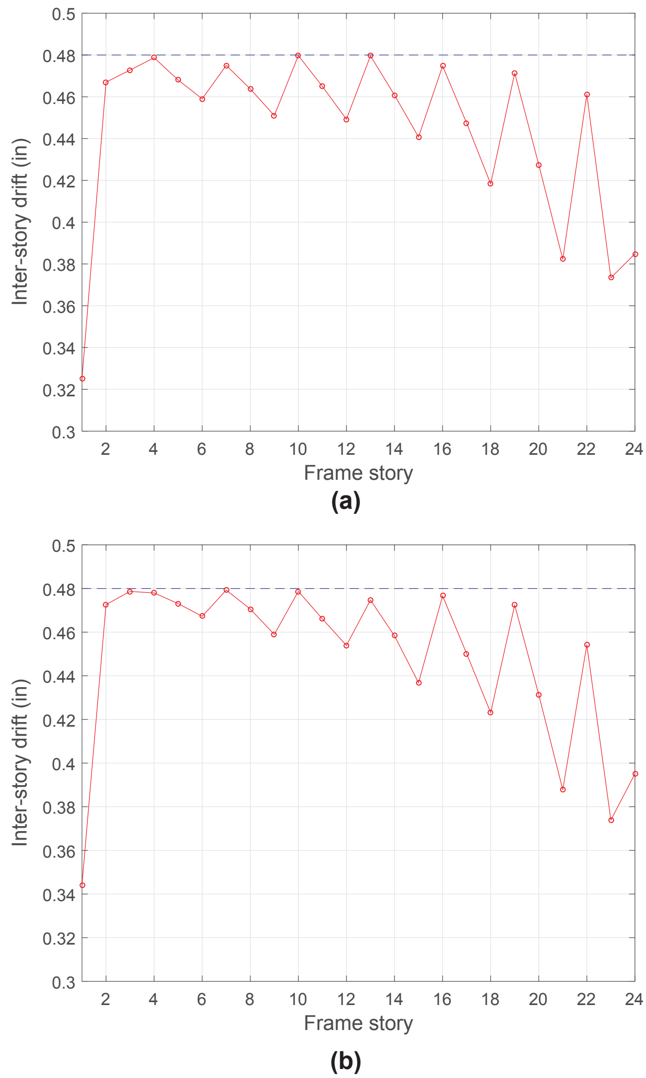

Fig. 10. Interstory drift for three-bay, twenty-four-story frame for (a) case 1 and (b) case 2.

$W = 5{,}761.85$ lb, $w_1 = 300$ lb/ft, $w_2 = 436$ lb/ft, $w_3 = 474$ lb/ft, and $w_4 = 408$ lb/ft [47]. The frame is designed following the AISC-LRFD specification [37] with a maximum interstory drift displacement constraint of (story height)/300. The material has a modulus of elasticity $E = 29{,}732$ ksi and a yield stress of $F_y = 33.4$ ksi. The effective length factors of the members are calculated as $K_x \geq 1.0$ for a sway-permitted frame using a simplified form of the transcendental equations [44] and the out-of-plane effective length factor is $K_y = 1.0$. All columns and beams are considered unbraced along their lengths.

Fabrication conditions are imposed on the construction of the 168-element frame requiring the same beam section be used in the first and third bays on all floors except the roof beams, resulting in 4 beam groups. Beginning at the foundation, the exterior columns are combined into a group and the interior columns are combined in another group, each over three consecutive stories, resulting in 16 column groups (see Fig. 7). Each of the 4 beam element groups are chosen from all 267 W-shapes, as listed in Table 1, while the 16 column element groups are limited to just the W14 sections (37 W-shapes). Fig. 7 shows the element group numbering scheme. The size of the resulting search space is approximately 6.27 (10^{34}) designs.

There are two approaches in the literature for analyzing this frame: Case 1 which includes the effects of shear stiffness and Case 2 where the shear stiffness is ignored. In this study, designs are generated for both cases and compared to other relevant optimization results reported in the literature.

Table 4 lists the SBO designs for both analysis cases and results using other optimization techniques. For Case 1, the best SBO design is a frame that weighs 216,306 lb., which is 1.9% lighter than the ACO design [21]. Over a 100 runs, the average weight is 224,310 lb., which is 2.3% smaller than that obtained with ACO. For Case 2, the best SBO design is a frame that weighs 202,422 lb. which between 0.35% and 5.8% lighter than other published designs. The average weight of the SBO designs is 209,560 lb. with a standard deviation equal to 7052 lb.

Fig. 8 shows convergence history plots for SBO for both analysis cases. Fig. 9 shows stress ratio values in all frame members for both cases; most elements are well below 60% of capacity and the highest stressed element is still less than 90% of capacity. Fig. 10 shows the interstory drift for both analyses cases for the best SBO frame design listed in Table 4. In both cases, the interstory drift constraint approaches the maximum values in the first column of each column group (group numbers 7, 8, 9, 10, 11 and 12). For this frame, interstory drift controls the design process; the strength requirements for both the beams and the columns are secondary considerations.

6. Summary

In this study, a school based optimization (SBO) algorithm is applied to the discrete design of steel frames. SBO takes advantage of numerous collaborative populations to enhance both the explorative and information sharing characteristics of the algorithm over other methods. The applied collaborative strategy in SBO can be easily implemented with any number of other metaheuristic algorithms to enhance their performance. In this study, TLBO is implemented with the SBO framework since the optimization algorithm has almost no adjustable parameters to influence and control its performance. The structural steel design problem is formulated as an optimization problem with the objective of minimizing the total frame weight. A penalty function is employed to enforce the strength and displacement constraints to the optimization problem as required by AISC-LRFD [37].

To demonstrate the efficiency of the SBO algorithm, three benchmark steel frame problems are designed and the results are compared with those of other optimization methods. Statistical results are provided based on 100 independent runs. SBO consistently developed lighter feasible designs than other optimization techniques. In addition, statistical results indicate the robustness and computational efficiency of SBO for the discrete optimization of steel frames.

References

[1] Ghasemi MR, Farshchin M. Pareto-based optimum seismic design of steel frames. Proc Inst Civ Eng-Struct Build 2014;167:66–74.
[2] Hayalioglu MS, Degertekin SO. Minimum cost design of steel frames with semi-rigid connections and column bases via genetic optimization. Comput Struct 2005;83:1849–63.
[3] Huang Y, Ludwig SA, Deng F. Sensor optimization using a genetic algorithm for structural health monitoring in harsh environments. J Civ Struct Health Monit 2016;6:509–19.
[4] Camp CV, Bichon BJ. Design of space trusses using ant colony optimization. J Struct Eng 2004;130:741–51.
[5] Ghasemi MR, Farshchin M. Ant colony optimisation-based multiobjective frame design under seismic conditions. Proc Inst Civ Eng-Struct Build 2011;164:421–32.
[6] Ghasemi MR, Farshchin M. Multi-objective weight and eigenperiod optimization of steel moment frames under seismic conditions, using ant colony method. In: Proc 8th World Congr. Struct. Multidiscip. Optim. WCSMO8; 2009.
[7] Kaveh A, Talatahari S. An improved ant colony optimization for the design of planar steel frames. Eng Struct 2010;32:864–73.
[8] Kaveh A, Hassani B, Shojaee S, Tavakkoli SM. Structural topology optimization using antcolony methodology. Eng Struct 2008;30:2559–65.
[9] Kaveh A, Maniat M. Damage detection based on MCSS and PSO using modal data. Smart Struct Syst 2015;15:1253–70.
[10] Doğan E, Saka MP. Optimum design of unbraced steel frames to LRFD–AISC using particle swarm optimization. Adv Eng Softw 2012;46:27–34.
[11] Kaveh A, Javadi SM, Maniat M. Damage assessment via modal data with a mixed particle swarm strategy, ray optimizer, and harmony search. Asian J Civ Eng BHRC

2014;15:95–106.
[12] Perez RE, Behdinan K. Particle swarm approach for structural design optimization. Comput Struct 2007;85:1579–88.
[13] Lee KS, Geem ZW. A new structural optimization method based on the harmony search algorithm. Comput Struct 2004;82:781–98.
[14] Lee KS, Geem ZW, Lee S, Bae K. The harmony search heuristic algorithm for discrete structural optimization. Eng Optim 2005;37:663–84.
[15] Kaveh A, Talatahari S. A novel heuristic optimization method: charged system search. Acta Mech 2010;213:267–89.
[16] Kaveh A, Maniat M. Damage detection in skeletal structures based on charged system search optimization using incomplete modal data. Int J Civ Eng IUST 2014;12:291–8.
[17] Kaveh A, Talatahari S. Optimal design of skeletal structures via the charged system search algorithm. Struct Multidiscip Optim 2010;41:893–911.
[18] Kaveh A, Maniat M, Naeini MA. Cost optimum design of post-tensioned concrete bridges using a modified colliding bodies optimization algorithm. Adv Eng Softw 2016;98:12–22.
[19] Kaveh A, Ilchi Ghazaan M. A comparative study of CBO and ECBO for optimal design of skeletal structures. Comput Struct 2015;153:137–47.
[20] Kaveh A, Ilchi Ghazaan M. Enhanced colliding bodies optimization for design problems with continuous and discrete variables. Adv Eng Softw 2014;77:66–75.
[21] Camp CV, Bichon BJ, Stovall SP. Design of steel frames using ant colony optimization. J Struct Eng 2005;131.
[22] Degertekin SO. Optimum design of steel frames using harmony search algorithm. Struct Multidiscip Optim 2008;36:393–401.
[23] Kaveh A, Talatahari S. Optimum design of skeletal structures using imperialist competitive algorithm. Comput Struct 2010;88:1220–9.
[24] Hasançebi O, Kazemzadeh Azad S. An exponential big bang-big crunch algorithm for discrete design optimization of steel frames. Comput Struct 2012;110–111:167–79.
[25] Kaveh A, Talatahari S. Charged system search for optimal design of frame structures. Appl Soft Comput 2012;12:382–93.
[26] Toğan V. Design of planar steel frames using teaching-learning based optimization. Eng Struct 2012;34:225–32.
[27] Kaveh A, Farhoudi N. A new optimization method: dolphin echolocation. Adv Eng Softw 2013;59:53–70.
[28] Maheri MR, Narimani MM. An enhanced harmony search algorithm for optimum design of side sway steel frames. Comput Struct 2014;136:78–89.
[29] Hasançebi O, Carbas S. Bat inspired algorithm for discrete size optimization of steel frames. Adv Eng Softw 2014;67:173–85.
[30] Talatahari S, Gandomi AH, Yang X-S, Deb S. Optimum design of frame structures using the eagle strategy with differential evolution. Eng Struct 2015;91:16–25.
[31] Carraro F, Lopez RH, Miguel LFF. Optimum design of planar steel frames using the Search Group Algorithm. J Braz Soc Mech Sci Eng 2016:1–14.
[32] Afzali SH, Darabi A, Niazkar M. Steel frame optimal design using MHBMO algorithm. Int J Steel Struct 2016;16:455–65.
[33] Kaveh A, Ghazaan MI. Enhanced whale optimization algorithm for sizing optimization of skeletal structures. Mech Based Des Struct Mach 2016:1–18.
[34] Yang X-S, Deb S. Two-stage eagle strategy with differential evolution. Int J Bio-Inspired Comput 2012;1;4(1):1–5.
[35] Farshchin M, Camp CV, Maniat M. Multi-class teaching learning-based optimization for truss design with frequency constraints. Eng Struct 2016;106:355–69.
[36] Farshchin M, Camp CV, Maniat M. Optimal design of truss structures for size and shape with frequency constraints using a collaborative optimization strategy. Expert Syst Appl 2016;66:203–18.
[37] LRFD-AISC Manual of steel construction, load and resistance factor design. 3rd ed., Chicago; 2001. n.d.
[38] Rao RV, Savsani VJ, Vakharia DP. Teaching–learning-based optimization: a novel method for constrained mechanical design optimization problems. Comput Aided Des 2011;43(3):303–15.
[39] Camp CV, Farshchin M. Design of space trusses using modified teaching–learning based optimization. Eng Struct 2014;62:87–97.
[40] Murren P, Khandelwal K. Design-driven harmony search (DDHS) in steel frame optimization. Eng Struct 2014;59:798–808.
[41] Brian R Wood, Adams Peter F, Beaulieu Denis. Column design by P Delta method. ASCE 1976;102:411–27.
[42] Camp C, Pezeshk S, Cao G. Optimized design of two-dimensional structures using a genetic algorithm. J Struct Eng 1998;124:551–9.
[43] Safari D, Maheri MR, Maheri A. Optimum design of steel frames using a multiple-deme GA with improved reproduction operators. J Constr Steel Res 2011;67:1232–43.
[44] Dumonteil P, Moore, W. Simple Equations for Effective Length Factors-Discussion. Eng J-Am Inst Steel Constr INC 1993; 30:37–37.
[45] Pezeshk S, Camp CV, Chen D. Design of nonlinear framed structures using genetic optimization. J Struct Eng 2000;126:382–8.
[46] Davison JH, Adams PF. Stability of braced and unbraced frames. J Struct Div 1974;100:319–34.
[47] Saka M, Kameshki E. Optimum design of unbraced rigid frames. Comput Struct 1998;69:433–42.